Experimental Robotics VII. The Fifth International Symposium,
Honolulu, HI, December 10-13, 2000, D. Rus and S. Singh, eds.,
Lecture notes in control and information sciences, Springer-Verlag.

Cooperative Human and Machine Perception in Teleoperated Assembly

Thomas Debus and Jeffrey Stoll
Boston University
Boston. MA
tdebus@bu.edu and jstoll@bu.edu

Robert D. Howe
Harvard University
Cambridge, MA
howe@deas.harvard.edu

Pierre Dupont
Boston University
Boston. MA
pierre@bu.edu

Abstract: This paper presents results on a teleoperator expert assistant – a system that in cooperation with a human operator estimates properties of remote environment objects in order to improve task performance. Specifically, an undersea connector-mating task is investigated in the laboratory using a PHANToM master and WAM remote manipulator. Estimates of socket orientation are obtained during task performance and conveyed to the operator through a graphical display. Task performance, measured by completion time and peak insertion force, is compared for operators using combinations of video images, the graphical display and a shared control mode in which the connector automatically rotates to the estimated socket orientation. The graphical display and automatic orientation controller reduce task completion times and contact forces by over one-third for inclined sockets when the video signal is noisy, e.g., due to water turbidity.

1 Introduction

At present, teleoperation is the only way that robots can perform sophisticated manipulation tasks in unstructured environments. In this control mode, the human operator performs all required sensing and planning, and generates all motion commands based on feedback from the remote environment. In practical teleoperation systems (e.g. undersea operations [1] and surgery [2]), the sensory feedback is often limited to video images without force feedback, which greatly restricts dexterity and productivity. We have been working to alleviate this situation by using information from the remote robot arm's sensors to assist in teleoperated manipulation tasks [3][4][5]. We have derived algorithms that identify essential properties of objects in the remote environment including geometry, mass, compliance, and friction.

In this paper, we focus on a specific practical application, undersea connector mating, where a cylindrical connector is inserted into a socket [1]. This peg-in-hole task is commonly performed in the offshore oil industry to provide hydraulic or electrical power to equipment on the sea floor. There are a number of factors that make this task troublesome. First, the clearance between the connector and receptacle is small, so a few degrees of angular misalignment can cause the connector to become jammed [6]. Second, sensory feedback is limited: because of stringent cost and reliability requirements, the master control device does not provide force feedback (Figure 1). Visual information is also restricted to monocular cameras that may be obstructed by sediment from nearby drilling operations. Third, manipulator arms for this application are hydraulically driven, with little compliance that would facilitate insertions. All these limitations make timely completion of this task difficult; in some cases it can take over an hour to insert a single connector, resulting in significant costs for the oil platform operator.

For a solution to find acceptance with the robot vendor and offshore operators, it must involve a minimum of modification to the robot, its controller and its software, as well as meeting rigorous reliability constraints. Thus, traditional robotic solutions to the insertion problem, such as mechanical or programmed remote center of compliance, are precluded. The ideal solution is one that can be implemented on an existing robot installation. Our proposed solution is to use the information from the joint angle sensors on the remote manipulator arm to determine the key geometric parameters of the remote environment. Specifically, we have developed an algorithm that automatically determines the relative orientation of the connector and the socket during the insertion task.

The process begins as the operator brings the connector into contact with the planar surface surrounding the opening of the socket, and slides the connector over the surface near the opening. The recorded joint sensor values are then combined with a model of the contact constraint between the cylindrical connector and the planar surface. Solution of the constraint equations yields a value for the orientation of the planar surface. This new information is presented to the operator as a graphical display to assist in orienting the connector. To explore the performance limitations imposed by the “minimum modification” rule, we have also implemented a shared control mode. In this approach, the connector is automatically oriented according to the estimated socket axis, while the operator controls translation to complete the insertion. This approach does not involve modification of the teleoperator system, but only access to joint encoder values. In this paper, we present experimental results confirming the benefits of the approach.

2 Methods

The laboratory teleoperator testbed used in these experiments consists of a PHANToM haptic interface as the master controller and a Barrett Whole Arm Manipulator (WAM) as the remote robot (Figure 2). To emulate the undersea application, the PHANToM (Model 1.5, Sensable Technologies, Cambridge, Mass., USA) is used as a passive 6 degree of freedom input device, and the motors are not activated. The WAM (Barrett Technologies, Cambridge, Mass., USA) is a redundant arm with 7 degrees of freedom, but only 5 axes are required for this insertion task, so the upper arm roll and final wrist roll axes are locked. Optical encoders measure the

joint position on both robots, and velocities are computed using filtered backward differences. The workspace is roughly 0.2 m in diameter for the master robot and 1.0 m in diameter for the remote robot. The WAM robot is controlled by a dedicated RISC processor (Model DS1103, dSpace GmbH, Paderborn, Germany) running at a 10 kHz servo rate. The PHANToM joint data is read by a PC at a rate of 1 kHz and written into memory shared by the PC and the RISC processor.

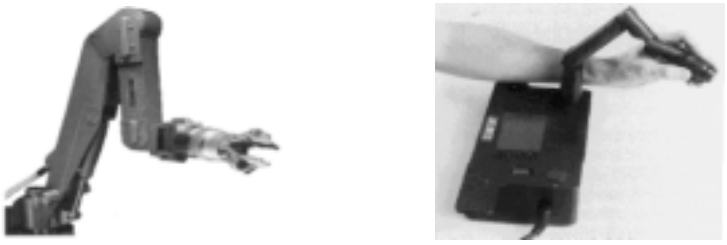

Figure 1. Schilling Robotic Systems Titan II manipulator, one of the leading commercial robots for undersea applications. (a) Remote manipulator arm is hydraulically powered. (b) The passive master arm provides no force feedback.

Figure 2. (a) WAM remote robot arm with connector mating apparatus. (b) PHANToM master arm.

Teleoperation is accomplished with a simple proportional-derivative controller with feedforward gravity and motor torque ripple compensation on the arm and integral feedback on the wrist. In this control method, incremental Cartesian position, velocity and orientation of the master robot are mapped to the remote workspace, converted to remote robot joint positions and velocity using inverse kinematics, and then to torque commands by the following control laws.

$$\begin{aligned} \tau_i^{\text{remote}} &= K_{Pi}(\theta_i^{\text{master}} - \theta_i^{\text{remote}}) + K_{Vi}(\dot{\theta}_i^{\text{master}} - \dot{\theta}_i^{\text{remote}}) + \tau_i^{\text{gravity}} + \tau_i^{\text{ripple}}, && \text{arm} \\ \tau_i^{\text{remote}} &= K_{Pi}(\theta_i^{\text{master}} - \theta_i^{\text{remote}}) + K_{Vi}(\dot{\theta}_i^{\text{master}} - \dot{\theta}_i^{\text{remote}}) + K_{Ii}\int(\theta_i^{\text{master}} - \theta_i^{\text{remote}})dt, && \text{wrist} \end{aligned} \quad (1)$$

Here $\theta_i, \dot{\theta}_i, \tau_i, \tau_i^{\text{gravity}}$ and τ_i^{ripple} are the i^{th} components of joint position, velocity, torque, gravity compensation and motor torque ripple compensation.

2.1 Environment modeling and operator assistance.

To find the orientation of the socket axis, we use techniques developed in our previous work [4],[5]. This approach estimates the remote object parameters by combining constraint equations describing the geometry of the contacting surfaces, closed loop kinematic relations, and kinematic data from the remote robot's joint sensors. In the present case, we are concerned with describing the contact point as the operator slides the cylindrical connector over the planar surface surrounding the socket. We assume that the connector is rigidly gripped by the remote robot in a known configuration. The contact point $p^{tool} = [x, y, z]^T$ on the connector is constrained to lie along its outer circular rim, which may be written in tool coordinates as

$$x^2 + y^2 - r^2 = 0, \quad z - l = 0 \tag{2}$$

where r and l are the known peg length and radius. The planar surface contact point $p^{world} = [u, v, w]^T$ may be written in world coordinates as

$$au + bv + cw + d = 0 \tag{3}$$

where *a*, *b*, *c*, and *d* are the desired parameters describing the orientation of the socket surface; we assume that the socket axis is normal to this surface, so that estimation of these parameters yields the correct connector orientation for insertion. These descriptions of the contact point *p* are related by the kinematic transformation between tool and world frames

$$T_{\text{world}}^{\text{tool}}(\theta)\, p^{\text{tool}} = p^{\text{world}} \tag{4}$$

As the connector slides over the planar surface, the joint positions θ are sampled, from which the transformation $T_{\text{world}}^{\text{tool}}(\theta)$ is calculated. Simultaneous solution of the above equations provides an estimate of the plane parameters *a*, *b*, *c*, and *d* and thus the correct connector orientation. This typically took 15 seconds to accomplish and 25 points were selected for the least squares estimation process using master-remote position error to infer contact.

The output is an estimate of the socket orientation for the insertion task. We are investigating a number of methods for conveying this information to the operator. The first is a 3D graphical model showing the manipulator, connector, and estimated plane location and orientation (Figure 3a), which is displayed on the monitor of the PHANToM–WAM interface computer. The model moves in real time to reflect the WAM's motion, and the operator can select the optimum rendering angle and distance. The second display shows a pair of targeting circles (Figure 3b). The larger circle represents the proximal end of the connector and the smaller circle the distal end, as projected onto the socket plane. The operator rotates the connector until the circles are concentric, which corresponds to the correct orientation, then proceeds with the insertion.

In addition to these displays, we have implemented a shared control mode. Following the estimation procedure, the orientation of the connector is automatically driven to the estimated socket angle, and orientation changes at the PHANToM stylus are ignored. The operator retains control of translational motion of the remote robot to perform the connector insertion. Additional display and shared control methods under development are described in the Discussion section below.

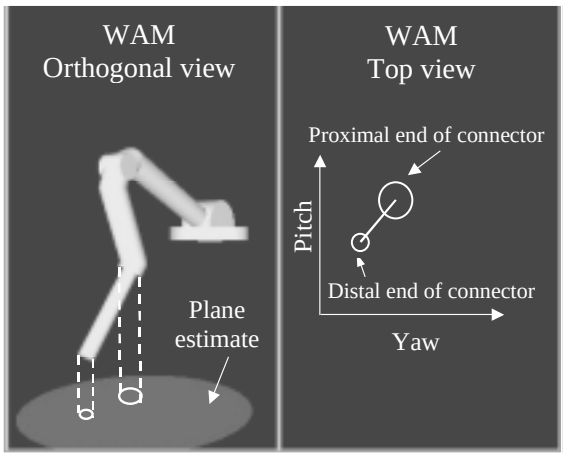

Figure 3. Graphical display (a) WAM model and (b) target circles, which are peg ends projected on the estimated socket plane.

2.2 Experimental protocol

The connector-socket apparatus was simulated by a pair of PVC plastic tubes (Figure 2a). The connector was 50 mm in diameter and 315 mm long. The socket had an inside diameter of 53 mm, and was mounted perpendicular to a planar surface that could be pivoted to a range of inclination angles between 0 and 57 degrees from horizontal. The operators used a monitor to view visual feedback from the remote robot via a video camera mounted adjacent to the shoulder joint of the WAM (Figure 4).

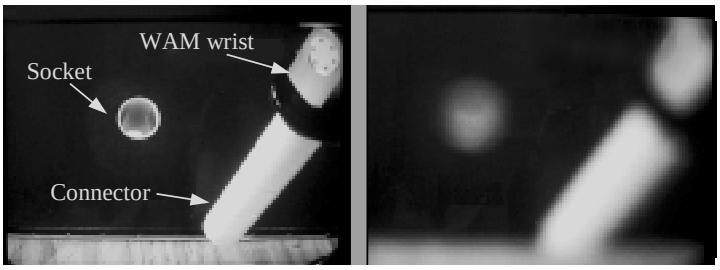

Figure 4. Typical visual feedback to operators from remote robot, showing the WAM wrist, connector, and socket opening. (a) Clear video signal. (b) Noisy video signal produced by defocusing video lens.

Two operators experienced in use of the system performed the insertion task under three different control modes and two visibility conditions, for a range of socket orientations. The first control mode provided only visual feedback with no estimation of the socket orientation, as in the current undersea connector mating task. The second mode added the two graphical displays of the estimated socket orientation described above, and the third used the shared control mode to automatically set the connector orientation in addition to the video and graphical displays. To simulate poor undersea visibility conditions, in some trials the video signal was degraded by defocusing, as shown in Figure 4(b). Each operator performed the task five times in each combination of control mode, visibility, and socket orientation.

In each trial that involved the estimation algorithm, the operator brought the end of the connector into contact with the planar surface surrounding the socket opening. The operator then depressed a switch that activated recording of joint angle data, and slid the connector over the surface. After releasing the switch, the operator proceeded with the insertion task. The time required for the estimation process and for the rest of the insertion task was recorded. In addition, the forces produced in the insertion process were approximated by recording the position errors at the remote robot and multiplying by the controller gain. This ignores inertial, impact, and frictional forces, but because of the clean drive train of the WAM robot and the quasi-static nature of the insertion task, it provides a reasonable estimate of the contact forces generated in the task.

3 Experiment results

In initial tests, we assessed the estimation algorithm's accuracy in determining the orientation of the planar surface around the socket opening. Five trials were conducted at five values of the orientation, at 0, 11, 30, 41 and 57 degrees. Figure 5 compares the estimated and actual orientations. These results show good agreement between the estimated and actual angles: the largest error is 1.3 degrees, and the largest standard deviation of the estimates at each angle is 0.6 degrees.

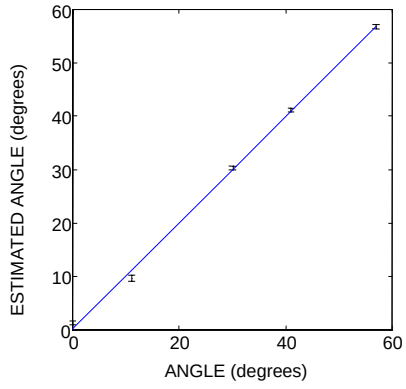

Figure 5. Estimates of the orientation of the planar surface around the socket opening.

Figure 6 and Figure 7 show the time-to-completion results for the connector-mating task for the three control modes and two visibility conditions at two surface orientations. For the two modes that used the estimation algorithm (i.e., graphic display and auto-orientation) separate results are indicated for the time to perform the estimate, the time to perform the insertion, and the sum of these, which is the total time to perform the task.

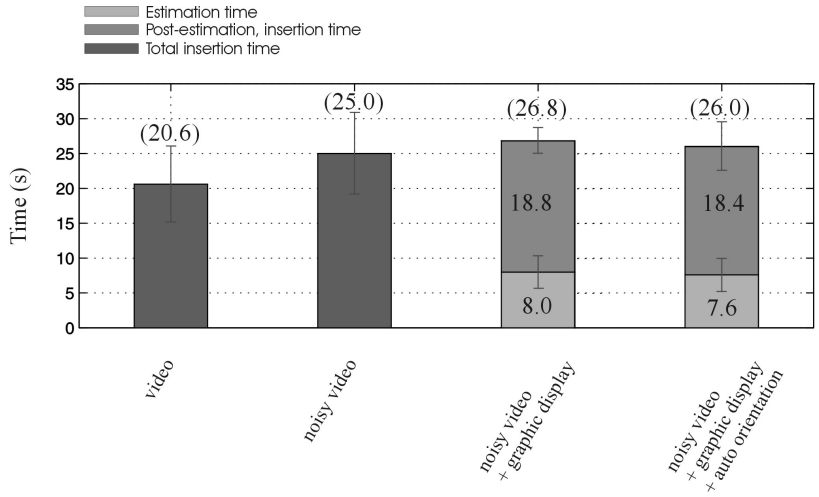

Figure 6. Task completion time as a function of control modes and visibility conditions for a horizontal surface. Symbols indicate mean; bars indicate standard deviations.

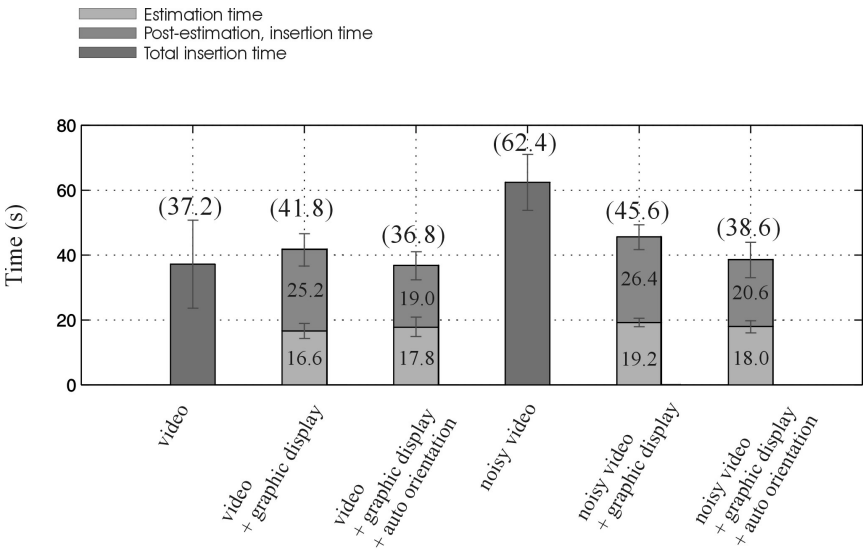

Figure 7. Task completion time as a function of control modes and visibility conditions for a surface inclined at 57 degrees.

As the angle of inclination was decreased from 57 degrees to horizontal, task completion time decreased uniformly. This is due to the assistance that gravity provides in correctly orienting the relatively compliant WAM wrist for a non-contact surface (Wrist compliance is due to tendon drive elasticity as well as deliberately reduced feedback gains, the latter in order to avoid damage-inducing contact forces). In addition, the steeper surface was less intuitive for the operators, especially during the estimation phase

These results indicate that, not surprisingly, the task takes significantly less time with clear video feedback. The more pertinent comparisons are within the clear and noisy video feedback conditions. With good visibility, task completion time is comparable with and without estimation algorithm. This is because executing the sliding motion that produces the data for the estimation algorithm takes approximately 40% of the task completion time. The insertion phase itself was 30-50% faster with either graphical or shared control assistance from the estimated angle compared to visual feedback only.

The effects of the estimation modes are more evident in the cases with poor visibility. With the socket plane inclined at 57 degrees, the entire task, including estimation and insertion, was 38% faster than when using visual information alone. For a horizontal socket plane, estimation increased total task time, while the insertion phase was considerably faster. For the non-zero inclination cases that used estimation, the shared control mode was uniformly faster than the graphic display mode.

Figure 8 shows estimates of the normalized peak force levels generated during the task for a socket plane inclined at 57 degrees. Normalization was based on video-only insertion force. As with the task completion time measure, the main difference of interest is among modes with poor visibility; the good visibility case produces the lowest forces. Both of the estimation-based modes produced peak forces over a third lower than the noisy video only mode.

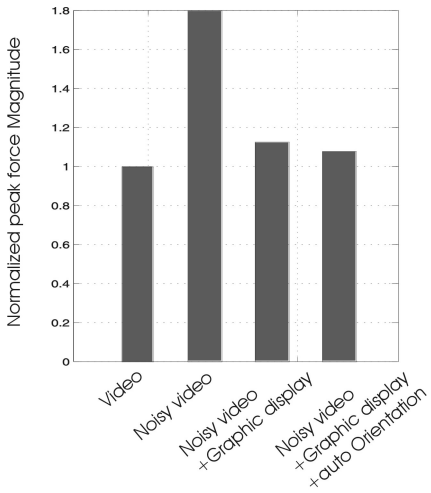

Figure 8. Normalized peak force estimates as a function of control mode for a socket plane inclined at 57 degrees.

4 Discussion

These results demonstrate that parameter estimation based on remote robot kinematic sensors can produce useful information for teleoperated manipulation tasks. Accuracy of surface orientation estimates was within 1.6 degrees, with a standard deviation of less than 0.6 degrees. Operators were able to accomplish the insertion phase of the task far more quickly with the estimation-based modes in all cases. These results indicate the viability of the technique and suggest a clear benefit for the intended application.

The approach has a number of features that make it well suited to the undersea application. The estimation algorithm is based on joint angle sensors only, which are standard components of the manipulators used in offshore applications. The algorithm does not require relatively expensive and fragile force sensing (although force information may improve the estimates and enable identification of additional properties [3]). This means that it is possible to configure a system that "looks over the shoulder" of the operator, without interfering with normal task execution and without significant modifications to the existing manipulator. If a graphical display is used to communicate with the operator, the computer that executes the estimation algorithm simply monitors the remote robot's joint sensors. If the estimation system fails, it has no impact on the manipulator's capabilities, so operations can continue as with the original manipulator system. This is an essential consideration for the offshore oil industry, where manipulator downtime can incur large costs.

Several important issues must be addressed prior to undersea implementation. One important issue is the difference in compliance between the WAM and undersea teleoperated robots, which are hydraulically powered, resulting in high endpoint impedance. High impedance makes insertions particularly difficult because the connector does not conform to contact forces and torques generated by misalignments. The relatively high compliance of the WAM resulted in much faster insertions than commonly observed in the undersea application. The low compliance of the hydraulic undersea manipulators makes the proposed estimation-based approach particularly beneficial, but it also makes it more difficult for the operator to slide the connector smoothly over the surface surrounding the socket. Further work will be directed at increasing the effective stiffness of the WAM arm to permit better investigation of these competing issues.

This application uses only a portion of the techniques we have developed for identifying the properties of remote environments during teleoperation [3],[4],[5]. In addition to estimating a variety of properties, these techniques can segment the data stream from the robot sensors and determine which contact states are active at each time. This enables a much greater range of applications. For example, the assumptions in the model, such as known length and radius of the connector, and perpendicular orientation between the socket axis and the surrounding surface, can be relaxed. A similar approach can be used to estimate other useful geometric parameters, such as the location of the socket opening. Such parameters can be presented to the operator using a variety of display modalities. Alternatively, they can be used to effect sophisticated shared controlled strategies. This capability promises to not only simplify teleoperation, but may represent a new level of perceptual capability for autonomous manipulation as well.

Acknowledgements

The support of the National Science Foundation under grant IIS-9988575 is gratefully acknowledged.

References

[1] Dennerlein J.T., Millman P., and Howe R.D. (1997). Vibrotactile Feedback for Industrial Telemanipulators. *Sixth Annual Symposium on Haptic Interfaces for Virtual Environment and Teleoperator Systems*, ASME International Mechanical Engineering Congress and Exposition, Dallas, Nov. 15-21, 1997, DSC-Vol. 61, pp. 189-195.

[2] Hill J.W, Jensen J.F. (1999). Telepresence technology in medicine: Principles and applications. *Proc. IEEE*, 86(3):369-380.

[3] Dupont P., Schulteis T., Millman P., and Howe R.D. (1999). Automatic Identification of Environment Haptic Properties. *Presence* 8(4):392-409.

[4] Debus T., Dupont P., and Howe R.D. (1999). Automatic Property Identification via Parameterized Constraints. *Proc. 1999 IEEE Conference on Robotics and Automation*, Detroit, MI, May, p. 1876-81.

[5] Debus T., Dupont P., and Howe R.D. (2000). Automatic Identification of Local Geometric Properties During Teleoperation. *Proc. 2000 IEEE Conference on Robotics and Automation*, San Francisco, CA, April, p. 3428-34.

[6] Whitney DE (1982). Quasi-Static Assembly of Compliantly Supported Rigid Parts, *ASME Journal of Dynamic Systems, Measurements, and Control* 104:65.